ARTICLES

Journal of Semiconductors
(2022) 43, 114101
doi: 10.1088/1674-4926/43/11/114101

Bulk GaN-based SAW resonators with high quality factors for wireless temperature sensor

Hongrui Lv[1, 2], Xianglong Shi[3], Yujie Ai[1, 2, †], Zhe Liu[1], Defeng Lin[1, 4], Lifang Jia[1], Zhe Cheng[1], Jie Yang[1], and Yun Zhang[1, 2, †]

[1]Institute of Semiconductors, Chinese Academy of Sciences, Beijing 100083, China

[2]Center of Materials Science and Optoelectronics Engineering, University of Chinese Academy of Sciences, Beijing 100049, China

[3]Beijing Aerospace Micro-electronics Technology Co., Beijing 100854, China

[4]Lishui Zhongke Semiconductor Material Co., Ltd., Lishui 323000, China

Abstract: Surface acoustic wave (SAW) resonator with outstanding quality factors of 4829/6775 at the resonant/anti-resonant frequencies has been demonstrated on C-doped semi-insulating bulk GaN. The impact of device parameters including aspect ratio of length to width of resonators, number of interdigital transducers, and acoustic propagation direction on resonator performance have been studied. For the first time, we demonstrate wireless temperature sensing from 21.6 to 120 °C with a stable temperature coefficient of frequency of –24.3 ppm/°C on bulk GaN-based SAW resonators.

Key words: surface acoustic wave; resonator; gallium nitride; quality factor; temperature sensor

Citation: H Lv, X L Shi, Y J Ai, Z Liu, D F Lin, L F Jia, Z Cheng, J Yang, and Y Zhang, Bulk GaN-based SAW resonators with high quality factors for wireless temperature sensor[J]. *J. Semicond.*, 2022, 43(11), 114101. https://doi.org/10.1088/1674-4926/43/11/114101

1. Introduction

Surface acoustic wave (SAW) wireless temperature sensors have the advantage of efficient and convenient information collection, as well as the ability to detect temperature in complex scenes, such as closed space, confined space and high-speed motion system. Therefore, they have been widely utilized for efficient online temperature monitoring for industrial equipment[1–3]. Thanks to high quality factor (Q > 5000) and low insertion loss (IL < 1 dB), quartz-based SAW resonators are usually adopted as temperature-sensitive elements for commercial wireless temperature sensors[4, 5]. However, quartz-based sensors can not be used at high temperature over 300 °C because of piezoelectric characteristics' degradation[6]. As a result, they are unable to meet the urgent demand for wireless temperature monitoring in high-temperature applications, such as aerospace engine turbines, oil and gas exploitation, and space exploration[6].

GaN exhibits good thermal stability of piezoelectric characteristics, and is considered as one of the most promising materials for SAW wireless sensors working at high temperatures over 500 °C[6–10]. Most reported SAW temperature sensors based on GaN are fabricated on GaN films grown on heterogeneous substrates. These GaN film-based sensors exhibited poor Q values lower than 2000, or large IL values higher than 5 dB due to the poor crystallization quality of films and acoustic loss between films and heterogeneous substrates[11–13]. It is difficult to demonstrate wireless temperature sensing function based on resonators with poor Q or large IL values. Therefore, until now, GaN-based SAW wireless temperature sensors have not been reported, and the reported GaN-based SAW sensors needed cables[8, 9].

It has been reported that the Q values of SAW resonators can be effectively improved by using bulk GaN instead of GaN films on heterogeneous substrates[14]. In this paper, bulk GaN-based SAW resonators with the highest Q values at both resonant and anti-resonant frequencies ever reported have been fabricated by a systematic study of the impact of device parameters on device performance. The Q values at the resonant and anti-resonant frequencies are as high as 4829 and 6775, respectively. The insertion loss at the resonant frequency is only 1.03 dB. The excellent Q values of bulk GaN-based resonators can be comparable with that of quartz-based resonators[4]. Moreover, we demonstrate wireless temperature sensing function based on these GaN-based SAW resonators for the first time, revealing great potential of GaN-based SAW resonators for wireless temperature sensing.

2. Experimental methods

Fig. 1(a) shows the schematic picture of one-port SAW resonators composed of interdigital transducers (IDTs) and a pair of reflectors. One-port SAW resonators were fabricated via electron beam evaporation and lift-off photolithography process on C-doped semi-insulating c-plane bulk GaN with a thickness of 400 μm. Ti/Al (10 nm/450 nm) film was deposited on the bulk GaN to form IDT electrodes. The acoustic wavelength (λ) is 8 μm and the metallization ratio of IDT electrodes is 50%, as shown in Fig. 1(b). To study the impact of the aspect ratio of length to width (L/W) of resonators with the same device area, the influence of the number of IDTs (N_{IDT}), and acoustic propagation direction on device perform-

Correspondence to: Y J Ai, aiyujie@semi.ac.cn; Y Zhang, yzhang34@semi.ac.cn

Received 18 APRIL 2022; Revised 15 MAY 2022.

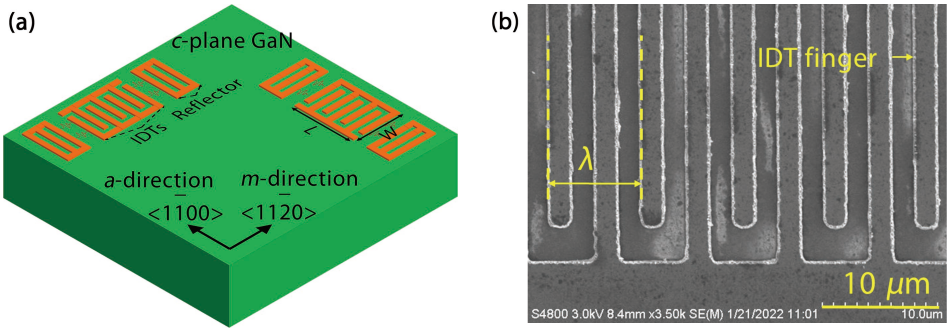

Fig. 1. (Color online) (a) Schematic picture of SAW resonators. (b) SEM image of IDT fingers.

Table 1. The performance of SAW resonators with different device parameters.

Sample	N_{IDT}	W	L/W	Direction	Q_{r_phase}	Q_{a_phase}	K_t^2 (%)
A	180	30λ	6	*m*	4829	6775	1.06
B	90	60λ	3/2	*m*	2825	2039	1.02
C	60	90λ	2/3	*m*	1883	532	0.86
D	45	120λ	3/8	*m*	808	423	0.72
E	90	30λ	3	*m*	2868	2269	0.83
F	360	30λ	12	*m*	3500	5690	0.75
G	180	30λ	6	*a*	1216	1764	0.39

ance, various devices with different parameters listed in Table 1 were fabricated. As shown in Fig. 1(a), the length (L) is defined by N_{IDT}λ, and the width is equal to the acoustic wave aperture (W). The Q_{r_phase}, Q_{a_phase}, and K_t^2 listed in Table 1 are the quality factor at the resonant frequency, quality factor at the anti-resonant frequency, and effective electromechanical coefficient of resonators, calculated by Eqs. (1), (2) and (5), respectively.

The crystal quality and surface morphology of bulk GaN are characterized by high resolution X-ray diffraction (HRXRD, Bede D1) and atomic force microscopy (AFM, Veeco D3100), respectively. The S parameters of devices were measured using a vector network analyzer (VNA, Keysight N5247B) after a standard TSOM (through, short, open, and match) calibration.

3. Results and discussions

Fig. 2(a) shows the 2θ–ω XRD scan pattern of bulk GaN. Two pronounced diffraction peaks at 2θ = 34.56° and 72.91° appear, corresponding to the hexagonal GaN (0002) plane and GaN (0004) plane, respectively. The GaN (0002) peak together with the detection of high-order GaN (0004) reflection attests to the high crystalline quality of the bulk GaN[15]. Figs. 2(b) and 2(c) present the XRD rocking curve of bulk GaN along $[0002]_{GaN}$ and $[10\bar{1}2]_{GaN}$, respectively. The full width at half maximum (FWHM) values of the XRD rocking curve of $[0002]_{GaN}$ and $[10\bar{1}2]_{GaN}$ peak are 41.86 and 46.27 arcsec, respectively. The bulk GaN exhibits a smooth surface morphology with a surface roughness of 0.184 nm, as shown in Fig. 2(d).

Figs. 3(a)–3(d) show the S_{11}, S_{21}, magnitude of input admittance ($|Y_{11}|$), and phase of input admittance of SAW-A with device parameters listed in Table 1, respectively. The Q values of the resonator are calculated by two methods. Q_{r_phase} and Q_{a_phase} are defined by Eqs. (1) and (2)[16]. Q_{r_3dB} and Q_{a_3dB} are defined by Eqs. (3) and (4)[17].

$$Q_{r\_phase} = \frac{f_r}{2} \cdot \left|\frac{d\phi}{df}\right|_{f_r}, \tag{1}$$

$$Q_{a\_phase} = \frac{f_a}{2} \cdot \left|\frac{d\phi}{df}\right|_{f_a}, \tag{2}$$

where f_r and f_a are the resonant and anti-resonant frequencies, respectively. $\left|\frac{d\phi}{df}\right|_{f_r}$ and $\left|\frac{d\phi}{df}\right|_{f_a}$ are the slopes of the phase of the Y_{11} with respect to f_r and f_a, respectively.

$$Q_{r\_3dB} = \frac{f_r}{\Delta f_{r\_3dB}}, \tag{3}$$

$$Q_{a\_3dB} = \frac{f_a}{\Delta f_{a\_3dB}}, \tag{4}$$

where Δf_{r_3dB} and Δf_{a_3dB} are 3-dB bandwidths of $|Y_{11}|$ at f_r and f_a, respectively. The effective electromechanical coefficient (K_t^2) is calculated by Eq. (5)[16]

$$K_t^2 = \frac{\pi}{4N} \cdot \frac{G(f_r)}{B(f_r)}, \tag{5}$$

where N is the number of IDT finger pairs, and $G(f_r)$ and $B(f_r)$ are the radiation conductance and susceptance deduced from input admittance.

SAW-A with device parameters listed in Table 1 exhibits the highest Q values of SAW resonators on bulk GaN ever reported at both f_r and f_a. The Q_{r_phase} and Q_{r_3dB} are 4829 and 4877 at 477.020 MHz, respectively. The Q_{a_phase} and Q_{a_3dB} are 6775 and 7455 at 477.161 MHz, respectively. The K_t^2 and insertion loss (IL) values of SAW-A are 1.06 % and 1.03 dB, respectively.

Table 1 shows the performance of SAW resonators with different design parameters. Among all the resonators fabricated, SAW-A with the number of IDTs (N_{IDT}) of 180, the acoustic wave aperture (W) of 30λ, and the acoustic propagation direction along *m*-direction of *c*-plane bulk GaN, exhibits the best device performance including Q_{r_phase}, Q_{a_phase}, and K_t^2. The device performance is improved as the value of L/W is increased from 3/8 (SAW-D) to 6 (SAW-A), due to the resist-

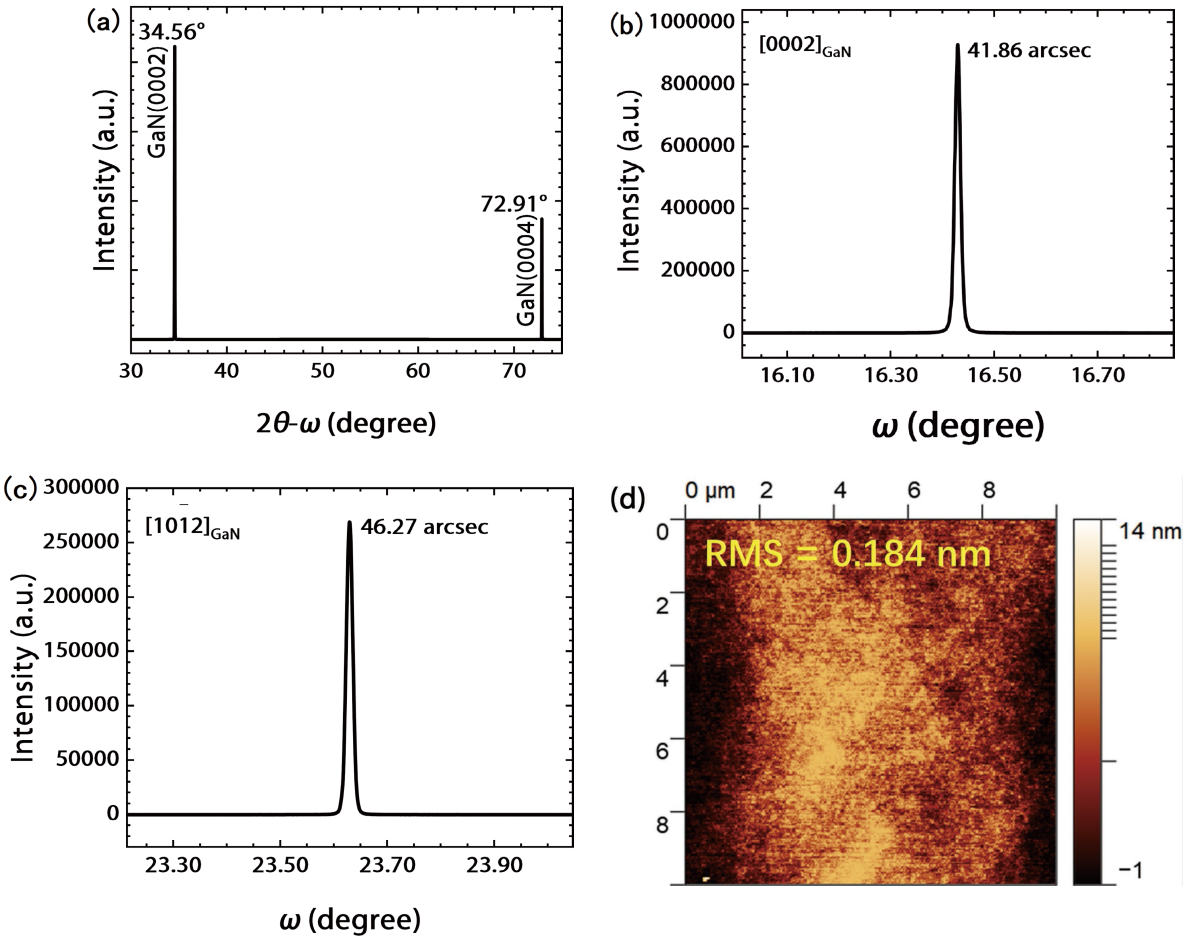

Fig. 2. (Color online) (a) 2θ–ω XRD scan patterns of bulk GaN. XRD rocking curves of bulk GaN along (b) $[0002]_{GaN}$ and (c) $[10\bar{1}2]_{GaN}$. (d) AFM image of bulk GaN in a range of 10×10 μm^2.

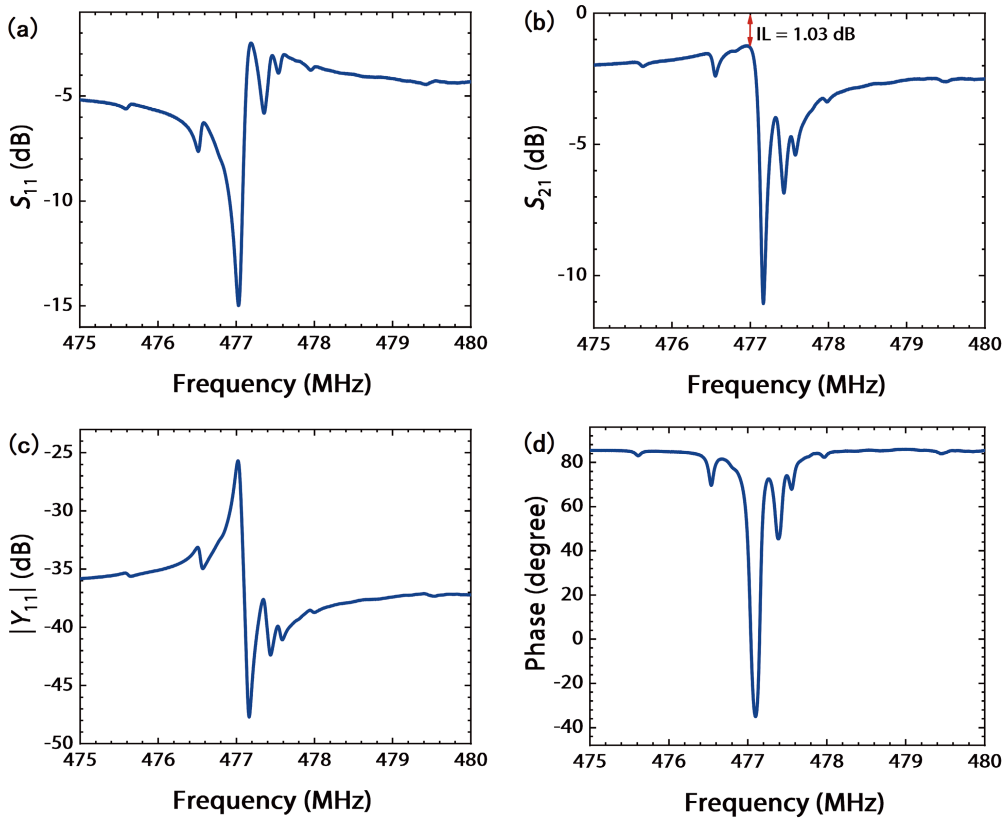

Fig. 3. (Color online) Frequency response (a) S_{11} and (b) S_{21} of the resonator, respectively. (c) Magnitude and (d) phase of input admittance of the resonator versus frequency.

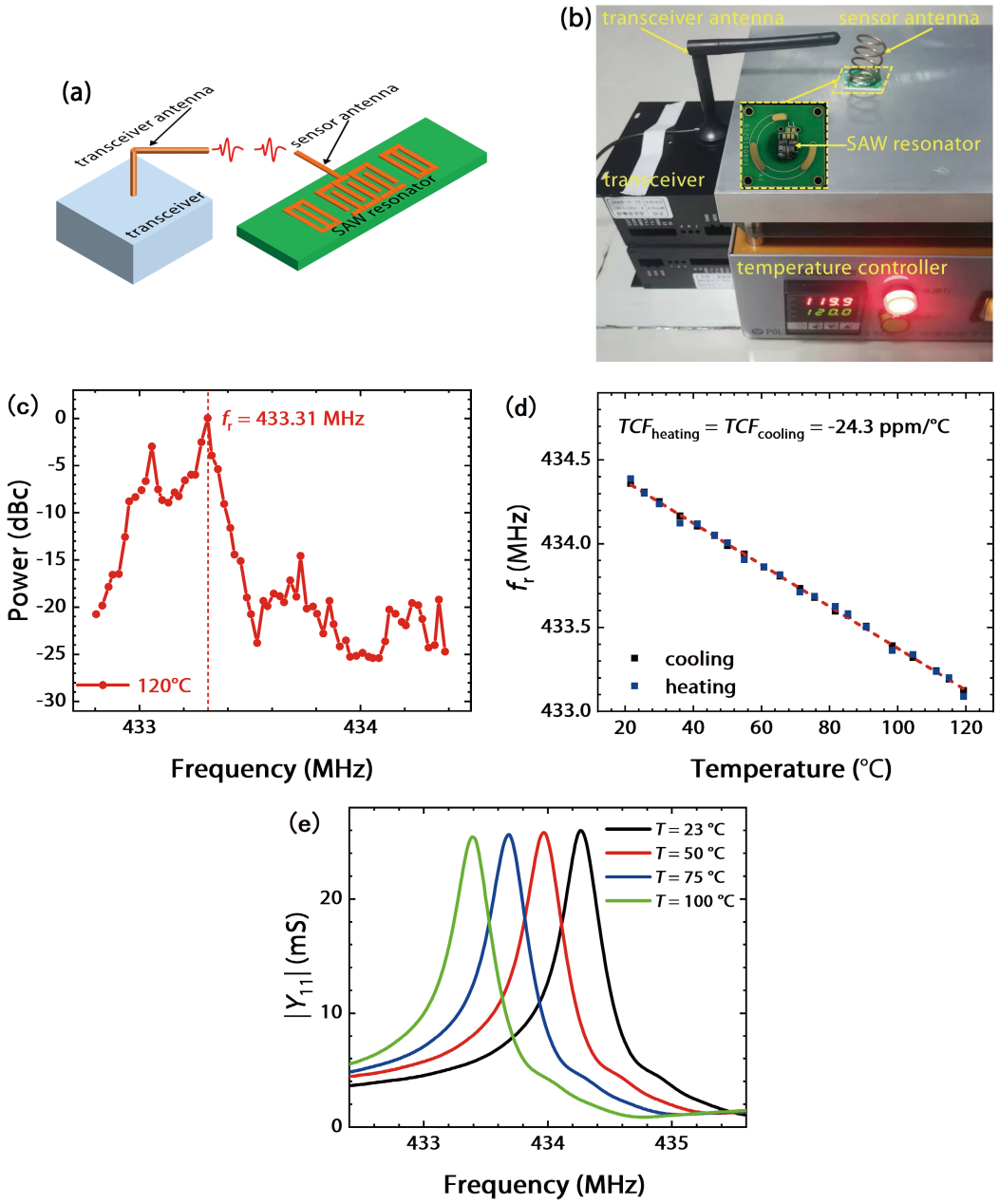

Fig. 4. (Color online) (a) Schematic diagram of the SAW wireless temperature sensor. (b) Setup of GaN-based SAW wireless temperature sensing system. (c) RF power distribution in the frequency domain received by the transceiver from the resonator at 120 °C. (d) Temperature dependency of f_r of GaN-based SAW wireless sensor during heating and cooling, respectively. (e) Admittance magnitude $|Y_{11}|$ of SAW sensors versus frequency with various temperatures from 23 to 100 °C.

ance reduction of IDTs with the increase of *L*/*W*. Compared with the resonators with N_{IDT} of 90 (SAW-E) and 360 (SAW-F), the resonator with N_{IDT} of 180 (SAW-A) shows the best device performance. The improved device performance with the increase of N_{IDT} from 90 to 180, can be attributed to strengthened acoustic energy with the increase of N_{IDT}. The degraded device performance with the further increase of N_{IDT} from 180 to 360, maybe attributed to that when N_{IDT} is very large, the resonator works more like a large capacitor[18]. Compared with the resonator along *a*-direction (SAW-G), the resonator with acoustic propagation direction along *m*-direction (SAW-A) exhibits better device performance[14].

Fig. 4(a) shows the schematic diagram of the SAW wireless temperature sensor, including a SAW resonator as a temperature sensitive element, an antenna connected to the SAW resonator, and a transceiver. The SAW resonator will resonant when the frequency of the RF signal transmitted by the transceiver is the same as the resonant frequency (f_r) of the resonator. As temperature changes, the f_r of the resonator changes due to the change of elastic stiffness[19], and the reflected signal from the SAW resonator will be fed back to the transceiver to extract the change of temperature according to the change of f_r[19]. Fig. 4(b) shows the setup of GaN-based SAW wireless temperature sensing system. A resonator with f_r of around 434 MHz and an acoustic wavelength of 8.8 μm is selected for wireless temperature sensing demonstration, because its f_r is located within the working frequency range of 425 to 475 MHz of commercial SAW wireless temperature sensors based on quartz-based resonators. The wireless communication distance between the antenna of the transceiver

and the resonator is 3 cm.

Fig. 4(c) shows the RF power distribution in the frequency domain received by the transceiver from the resonator at 120 °C. The frequency of the RF signal with the highest power, corresponding to the f_r of the resonator is 433.31 MHz at 120 °C. Fig. 4(d) shows the temperature dependency of f_r of the resonator measured by the setup shown in Fig. 4(b). The f_r of the SAW sensor varies linearly with temperature as the temperature increases from 21.6 to 120 °C and then decreases to 21.6 °C with a temperature coefficient (TCF) of −24.3 ppm/°C. The TCF of the sensor is defined by Eq. (6)[20].

$$\mathrm{TCF} = \frac{1}{T - T_0} \cdot \frac{f(T) - f(T_0)}{f(T_0)}, \tag{6}$$

where T is the temperature in Celsius, $f(T)$ is the resonance frequency at T, and T_0 is 25 °C. Fig. 4(e) shows the admittance magnitude $|Y_{11}|$ of the SAW sensor versus frequency with various temperatures from 23 to 100 °C. The $|Y_{11}|$ of the f_r at 23, 50, 75, and 100 °C are 25.992, 25.787, 25.547, and 25.430 mS, respectively. The result shows that, as the temperature is increased from 23 to 100 °C, the reduction of admittance at the f_r is only about 2.2 %. This indicates that it is the working temperature of other supplementary elements, such as the inductor for matching and PCB that we adopted, that limits the working temperature of the wireless temperature sensor that we demonstrate.

4. Conclusions

In conclusion, we have reported the highest Q values of bulk-GaN based SAW resonators at both the resonant and anti-resonant frequencies. The Q values at resonant/anti-resonant frequencies are 4829/6775, respectively. The impact of device parameters including L/W, N_{IDT}, and acoustic propagation direction on the performance of resonators have been studied. The results indicate that the increase of L/W value from 3/8 to 6, set N_{IDT} to be 180 rather than 90 and 360, and set the acoustic propagation direction to be m-direction rather than a-direction favor the improvement of Q and K_t^2 values of SAW resonators on c-plane bulk GaN substrate. Moreover, we have demonstrated the wireless temperature sensing from 21.6 to 120 °C with a TCF of −24.3 ppm/°C based on bulk GaN-based SAW resonators for the first time.

Acknowledgements

The research is supported by the National Natural Sciences Foundation of China (Grant No. 61974137), and the One Hundred Person project of the Chinese Academy of Science.

References

[1] Wang W, Xue X, Fan S, et al. Development of a wireless and passive temperature-compensated SAW strain sensor. Sens Actuators A, 2020, 308, 112015

[2] Li B, Yassine O, Kosel J. A surface acoustic wave passive and wireless sensor for magnetic fields, temperature, and humidity. IEEE Sensors J, 2014, 15(1), 453

[3] Bao X Q, Burkhard W, Varadan V V. et al. SAW Temperature sensor and remote reading system. IEEE 1987 Ultrasonics Symposium, 1987, 583

[4] Avramov I D, Suohai M. Surface transverse waves exceed the material Q limit for surface acoustic waves on quartz. IEEE Trans Ultrason, Ferroelectrics, Frequency Control, 1996, 43(6), 1133

[5] Ballandras S, Lardat R, Penavaire L, et al. P1i-5 micro-machined, all quartz package, passive wireless saw pressure and temperature sensor. 2006 IEEE Ultrasonics Symposium, 2006, 1441

[6] Hornsteiner J, Born E, Fischerauer G, et al. Surface acoustic wave sensors for high-temperature applications. Proceedings of the 1998 IEEE International Frequency Control Symposium, 1998, 615

[7] Hassan A, Savaria Y, Sawan M. GaN integration technology, an ideal candidate for high-temperature applications: A review. IEEE Access, 2018, 6, 78790

[8] Müller A, Konstantinidis G, Buiculescu V, et al. GaN/Si based single SAW resonator temperature sensor operating in the GHz frequency range. Sens Actuators A, 2014, 209, 115

[9] Qamar A, Eisner S R, Senesky D G, et al. Ultra-high-Q gallium nitride SAW resonators for applications with extreme temperature swings. J Microelectromechan Syst, 2020, 29(5), 900

[10] Son K, Liao A, Lung G, et al. GaN-based high temperature and radiation-hard electronics for harsh environments. Nanosci Nanotechnol Lett, 2010, 2(2), 89

[11] Bartoli F, Aubert T, Moutaouekkil M, et al. AlN/GaN/Sapphire heterostructure for high-temperature packageless acoustic wave devices. Sens Actuators A, 2018, 283, 9

[12] Müller A, Konstantinidis G, Giangu I, et al. GaN-based SAW structures resonating within the 5.4–8.5 GHz frequency range, for high sensitivity temperature sensors. 2014 IEEE MTT-S International Microwave Symposium, 2014, 1

[13] Müller A, Konstantinidis G, Stefanescu A, et al. Pressure and temperature determination with micromachined GAN/SI SAW based resonators operating in the GHZ frequency range. 2017 19th International Conference on Solid-State Sensors, Actuators and Microsystems, 2017, 1073

[14] Ji X, Dong W X, Zhang Y M, et al. Fabrication and characterization of one-port surface acoustic wave resonators on semi-insulating GaN substrates. Chin Phys B, 2019, 28(6), 067701

[15] Kushvaha S S, Kumar M S, Maurya K K, et al. Highly c-axis oriented growth of GaN film on sapphire (0001) by laser molecular beam epitaxy using HVPE grown GaN bulk target. AIP Adv, 2013, 3(9), 092109

[16] Li Q, Qian L, Fu S, et al. Characteristics of one-port surface acoustic wave resonator fabricated on ZnO/6H-SiC layered structure. J Phys D, 2018, 51(14), 145305

[17] Zou J. High quality factor Lamb wave resonators. EECS Department University of California, Berkeley Technical Report No. UCB/EECS-2014-217, 2014

[18] Lv H R, Huang Y L, Ai Y J, et al. An experimental and theoretical study of impact of device parameters on performance of AlN/sapphire-based SAW temperature sensors. Micromachines, 2021, 13(1), 40

[19] Elmazria O, Aubert T. Wireless SAW sensor for high temperature applications: Material point of view. In: Smart Sensors, Actuators, and MEMS V. SPIE, 2011, 8066, 19

[20] Dong W, Ji X, Huang J, et al. Sensitivity enhanced temperature sensor: one-port 2D surface phononic crystal resonator based on AlN/sapphire. Semicond Sci Technol, 2019, 34, 055005

Hongrui Lv got his BS from Shandong University in 2015. Now he is a PhD student at Institute of Semiconductors, University of Chinese Academy of Sciences under the supervision of Prof. Yujie Ai. His research focuses on nitride-based surface acoustic wave (SAW) wireless temperature sensors.

Yujie Ai got his BS degree in 2004 at Shandong Normal University and PhD degree in 2011 at Peiking University. He joined Institute of Semiconductors, Chinese Academy of Sciences as a full professor. His research interests include acoustic filters and sensors.

Yun Zhang got his BS degree in 2005 at Tsinghua University and Ph.D. degree in 2011 at Georgia Institute of Technology. He joined Institute of Semiconductors, Chinese Academy of Sciences as a full researcher. His research interests are wide-bandgap semiconductor materials and devices including UV optoelectronic devices, RF devices, power electronic devices and related integrated circuits.